

Understanding Fact Recall in Language Models: Why Two-Stage Training Encourages Memorization but Mixed Training Teaches Knowledge

Ying Zhang¹ Benjamin Heinzerling^{1,2} Dongyuan Li³

Ryoma Ishigaki^{4,5} Yuta Hitomi⁵ Kentaro Inui^{1,6}

¹RIKEN Center for Advanced Intelligence Project ²Tohoku University

³The University of Tokyo ⁴Tokyo Denki University ⁵Alt Inc ⁶MBZUAI

Correspondence: ying.zhang@riken.jp

Abstract

Fact recall, the ability of language models (LMs) to retrieve specific factual knowledge, remains a challenging task despite their impressive general capabilities. Common training strategies often struggle to promote robust recall behavior with two-stage training, which first trains a model with fact-storing examples (e.g., factual statements) and then with fact-recalling examples (question-answer pairs), tending to encourage rote memorization rather than generalizable fact retrieval. In contrast, mixed training, which jointly uses both types of examples, has been empirically shown to improve the ability to recall facts, but the underlying mechanisms are still poorly understood. In this work, we investigate how these training strategies affect how model parameters are shaped during training and how these differences relate to their ability to recall facts. We introduce *cross-task gradient trace* to identify *shared parameters*, those strongly influenced by both fact-storing and fact-recalling examples. Our analysis on synthetic fact recall datasets with the Llama-3.2B and Pythia-2.8B models reveals that mixed training encouraging a larger and more centralized set of shared parameters. These findings suggest that the emergence of parameters may play a key role in enabling LMs to generalize factual knowledge across task formulations¹.

1 Introduction

If someone knows that “Barack Obama was born in Hawaii,” they should easily answer the question, “Where was Barack Obama born?” We refer to this process of answering questions using previously acquired knowledge as *fact recall*. Fact recall is an important capability involved in many aspects of language understanding, but is a challenging problem for LMs trained via next-token prediction based on word co-occurrence [17, 48], as this objective encourages *rote memorization*. For example, a model trained on “Barack Obama was born in Hawaii” can predict “Hawaii” when prompted with “Barack Obama was born in,” but fails on “Where was Barack Obama born?” [3]. This differs from human fact recall, which naturally involves a deeper understanding to abstract the entities “Barack Obama” and “Hawaii” and identify their relation “was born in.”

Recent work has explored how LMs store and recall facts via specific neurons and attention patterns [10, 15, 19, 20, 25, 33, 37, 38], and has developed training strategies to improve fact recall [3, 21, 29]. Notably, [3] show that *two-stage training*, which first trains on fact-storing (e.g., factual statements) and then on fact-recalling (question-answer pairs), primarily leads to rote memorization characterized by very low (9.7%) fact recall accuracy on unseen questions. In contrast,

¹Our code will be available at Github.

mixed training, which mixes fact-storing and fact-recalling examples, helps the model learn facts as generalizable knowledge that can be retrieved across different query forms. We refer to this ability as teaching knowledge, which is evidenced by a much higher accuracy (88.6%) in fact recall. While promising, this raises key questions: ① *Why does two-stage training appear to encourage memorization while mixed training appears to teach knowledge?* ② *How does this factor internally support the model after mixed training for fact recall?* This study provides an explanation to these questions. For Question ①, we identify that a small subset of model parameters, termed *shared parameters* (fewer than 2% of all parameters), are influenced by both fact-storing and fact-recalling examples. The impact of these examples on shared parameters varies significantly between mixed training and two-stage training, resulting in distinct distributions of these parameters, which in turn lead to substantial variations in model performance on fact recall (§ 3). For Question ②, we reveal that, in mixed training, shared parameters support fact recall by concentrating within critical attention heads, while these heads effectively function as switches to activate the fact recall mechanism (§ 4).

In detail, we applied both mixed training and two-stage training to fine-tune two LMs: Llama-3.2-3B [2] and Pythia-2.8B [7], using biographical statements (BIO) for fact-storing and question-answer pairs (QA) for fact-recalling. For Question ①, we propose a tool called *cross-task gradient trace*. This tool uses gradient attribution [5] to identify parameters that are strongly influenced by both BIO and QA examples during backpropagation; we refer to these as *shared parameters*. Mixed training yields more shared parameters than two-stage training, and ablating them results in a much larger performance drop. For example, in Llama, the shared set is 1.2 times larger under mixed training, and ablating it reduces QA accuracy from 74.7 to 8.7, compared to a smaller drop from 35.9 to 29.2 under two-stage training. These findings highlight the central role of shared parameters in enabling generalizable fact recall. To further investigate this, we identify *fact recall-related parameters*, which recover fact recall with a minimal set of parameters. Mixed training achieves a more efficient trade-off between the number of these parameters and the performance they recover. Notably, ablating shared parameters from this critical set leads to a larger performance drop under mixed training, indicating that shared parameters are key to this efficiency. For Question ②, we further analyze their distribution in critical attention heads. Experimental results show that, over 60% shared parameters in attention heads are concentrated in the top 10% of heads. Ablating these heads leads to a 90% drop in fact recall. A case study provides qualitative insight: in the Mix-tuned model, shared parameters encourage the top-ranked head to develop reusable mechanisms across fact-storing and fact-recalling examples.

These findings reveal **how mixed training teaches knowledge by increasing the quantity and collective importance of shared parameters, which are concentrated in critical attention heads for fact recall**. Our work sheds light on how mixed training influences the internal mechanisms of LMs and introduces a new tool, the cross-task gradient trace, for interpreting neural networks.

2 Preliminaries

2.1 Preliminary Backgrounds

Factual Knowledge: We define a fact as a triple (s, r, a) that maps a subject entity s and a relation type r to an attribute a . For example, $(Barack\ Obama, wasBornOn, August-4-1961)$. We present each fact in two natural language formats: a *biographical statement* (BIO) and a *question-answer* pair (QA). In the BIO format, the fact is expressed as a declarative sentence (e.g., *Barack Obama’s life journey began on August 4, 1961*). In the QA format, the fact is expressed as a question about the subject, with the attribute as the answer (e.g., *Q: What is the birth date of Barack Obama? A: August 4, 1961*). **Fact Recall:** In fact recall tasks, when asked a question about a subject-relation pair (s, r) , the model needs to recall the corresponding fact and output the attribute a [20, 25].

2.2 Preliminary Experiments

Experimental Setup. To ensure a clean analysis and avoid interference from pre-existing factual knowledge in LMs, we constructed synthetic BIO and QA datasets following the procedure of [3], both covering the same 10,000 unique individuals. For the QA dataset, 5,000 individuals were used for model training, forming the QA *in-distribution* set, while the remaining 5,000 were held out for evaluation, forming the QA *out-of-distribution* set. See Appendix A.2 for further details. We analyze two decoder-only LMs based on the Transformer architecture: Llama-3.2 (28 layers, 3B parameters) and Pythia (32 layers, 2.8B parameters). While Llama uses a 128K vocabulary, Pythia uses a 50K

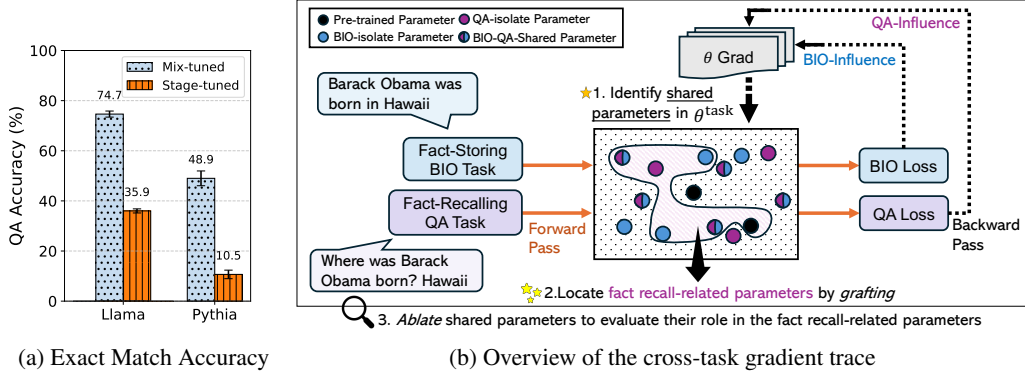


Figure 1: (a) **Performance of fine-tuned Llama and Pythia on QA out-of-distribution set.** The Mix-tuned model substantially outperforms the Stage-tuned model, demonstrating superior generalization in the fact recall task. (b) **Overview of the proposed tool.** The fine-tuned model (θ^{task}) first performs a forward pass to compute task-specific loss. During the backward pass (i.e., backpropagation), we track gradients for each parameter (θ) and identify *shared parameters*—those strongly influenced by both BIO and QA tasks. After fine-tuning, we apply *grafting* to locate fact recall-related parameters and perform *ablation* to evaluate the role of shared parameters in this subset.

vocabulary. Each Transformer layer consists of a multi-head self-attention (MHA) module and an MLP block. Pythia computes the MHA and MLP components in parallel, whereas Llama uses the standard sequential design. All experimental results are averaged over 3 random seeds. Please note that all downstream experiments presented in Sections 3 and 4 follow these experimental settings. Reported error bars represent the standard deviation (1-sigma) across these three runs.

Experimental Findings. We investigate two fine-tuning strategies differing in training order: (1) *Two-Stage Training*. We first fine-tune the pre-trained LM on the BIO dataset alone, allowing it to memorize the biographical statements. We then fine-tune this model on the QA in-distribution dataset to adapt it to the question-answer format. The result is a *Stage-tuned* model. (2) *Mixed Training*. We fine-tune the pre-trained LM on a mixed dataset containing all BIO statements combined with the QA in-distribution examples. BIO and QA examples are randomly shuffled into training batches. The resulting model is referred to as the *Mix-tuned* model. See Appendix A.3 for detailed fine-tuning procedures. After training, we evaluate the Stage-tuned and Mix-tuned models on the QA out-of-distribution data. We report exact match accuracy as the evaluation metric, treating the input prefix as the prompt and evaluating the predicted attribute span. Figure 1 (a) summarizes the performance. The Mix-tuned model outperforms the Stage-tuned model by over 38 points in accuracy, demonstrating superior generalization. Figure 6 in Appendix A.3 further confirms that both models successfully store BIO statements and adapt to QA in-distribution, indicating that the performance gap lies in extracting underlying knowledge. These results indicate that two-stage training encourages rote memorization, while mixed tuning teaches knowledge. In the following section, we investigate the internal differences between fine-tuned models that account for this performance gap.

3 Explaining fact recall differences with cross-task gradient trace: how shared parameters matter

To answer our first question—*why does two-stage training appear to encourage memorization while mixed training appears to teach knowledge?*—we analyze this from the perspective of parameter evolution during fine-tuning. We hypothesize that the performance gap between two-stage and mixed training arises from differences in how they optimize parameters. Specifically, in two-stage training, the model is first fine-tuned on BIO data and then separately on QA data. Because these two phases are decoupled, parameters optimized in the first phase are not necessarily revisited or reinforced in the second. As a result, some parameters are primarily optimized during the BIO phase, referred to as BIO-isolate parameters, and remain largely unchanged during the subsequent QA phase. Similarly, the QA phase primarily optimizes a different set of parameters, referred to as QA-isolate parameters. Consequently, only a small subset of parameters is jointly optimized by both tasks, which we refer to as *shared parameters*. In contrast, mixed training fine-tunes the model on BIO and QA examples

simultaneously, aiming to minimize a combined loss. Faced with limited training data and parameter capacity, the model naturally reuses and refines a subset of parameters that are useful for both tasks. Through more frequent and consistent optimization, these shared parameters are potentially better suited to capturing patterns relevant to both BIO and QA than BIO- or QA-isolate parameters. This helps explain why mixed training improves fact recall and motivates our focus on shared parameters.

To investigate this hypothesis, as shown in Figure 1 (b), we introduce the *cross-task gradient trace*, a method for identifying and analyzing shared parameters. Section 3.1 describes how we define and identify these shared parameters using gradient information. Section 3.2 further examines their differences between mixed and two-stage trainings in supporting fact recall.

3.1 Defining and identifying shared parameters: revealing their impact on fact recall

In this section, we formally define shared parameters and describe how they are identified using gradient signals obtained during backpropagation. We then demonstrate their direct impact on fact recall through empirical evaluation.

Definition 3.1 (Shared Parameters). We define **shared parameters** (\mathcal{S}) as top- k model parameters significantly influenced by **both** the BIO and QA tasks. To quantify the influence Δ_i^{task} of a task on a parameter θ_i , we measure how much θ_i changes when fine-tuned on specific examples. A parameter θ_i is considered **shared** if both its BIO-influence Δ_i^{BIO} and QA-influence Δ_i^{QA} are large.

We calculate Δ_i^{task} based on the mechanics of backpropagation [5]. Given a training dataset $\mathcal{D}_{\text{task}}$, after training on a single example $d_n \in \mathcal{D}_{\text{task}}$, the parameter θ_i is updated as:

$$\theta_i \leftarrow \theta_i + \text{lr}(d_n) \times \text{grad}_i^{\text{task}_n}, \quad (1)$$

where $\text{lr}(d_n)$ is the learning rate at that step, and $\text{grad}_i^{\text{task}_n}$ is the gradient of the task-specific loss on example d_n with respect to θ_i . A large gradient magnitude $|\text{grad}_i^{\text{task}_n}|$ suggests that the parameter is significantly influenced by that training step. Summing these updates across the entire dataset provides the total influence of the task on θ_i :

$$\Delta_i^{\text{task}} = \sum_{d_n \in \mathcal{D}_{\text{task}}} \text{lr}(d_n) \times \text{grad}_i^{\text{task}_n}. \quad (2)$$

To determine which parameters are most influenced by each task, we rank all parameters in descending order of Δ_i^{BIO} and Δ_i^{QA} . The top- k parameters for each task are considered the most influenced by that task. Parameters appearing in both the BIO and QA top- k sets are identified as shared parameters.

Mathematically, let $\text{rank}_{\text{task}}(i)$ denote the rank of Δ_i^{task} (with rank 1 being the highest influence). We define the top- k influenced parameters for a given task as:

$$\mathcal{A}_{\text{task}} = \{\theta_i \mid \text{rank}_{\text{task}}(i) \leq k\}. \quad (3)$$

The shared parameter set is the intersection of the BIO and QA top- k sets. To account for distributional differences between the BIO and QA training sets, we further partition the BIO data into in-distribution and out-of-distribution subsets based on their corresponding QA individuals. We then apply the same ranking procedure separately for these subsets, resulting in two types of shared parameters:

$$\mathcal{S}_{\text{I}} = \mathcal{A}_{\text{BIO_in}} \cap \mathcal{A}_{\text{QA_in}}, \quad \mathcal{S}_{\text{II}} = \mathcal{A}_{\text{BIO_out}} \cap \mathcal{A}_{\text{QA_in}}. \quad (4)$$

We measure the impact of the identified shared parameters on fact recall by observing the effect of ablating them from the fine-tuned model. Specifically, we reset the values of shared parameters in the fine-tuned model to their pre-trained values while keeping all other parameters unchanged. Parameters that are unnecessary for the task should not significantly impact final performance [32, 9].

Experimental Setup. Directly computing Δ_i^{task} for all parameters across the full dataset is computationally expensive. Therefore, we estimated these influence values using a subset of training data consisting of 20 individuals. For \mathcal{S}_{I} , we used 10 individuals shared between BIO_in and QA_in. For \mathcal{S}_{II} , we used the same 10 QA_in individuals and a different set of 10 individuals from BIO_out. During fine-tuning, we recorded parameter gradients for these 20 individuals using PyTorch’s `torch.autograd.grad` function. By varying k in the range $[10, 10^8]$, we tracked the proportion of shared parameters among the top- k most influenced parameters, denoted as $\frac{|\mathcal{S}|}{k}$.

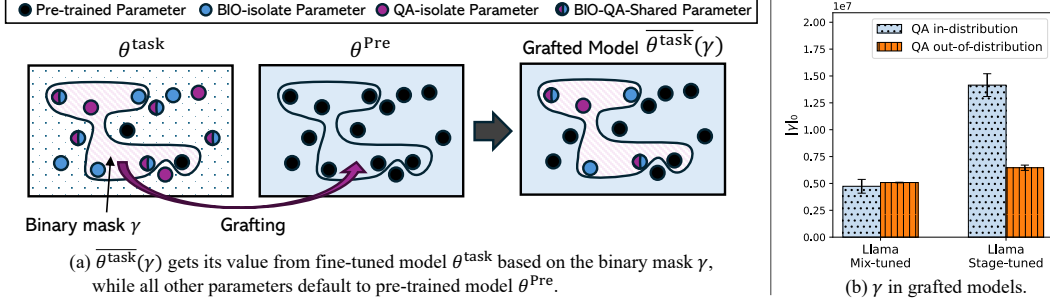


Figure 3: (a) Grafting procedure. (b) Number of fact recall-related parameters ($|\gamma|_0$) in grafted models. Mix-tuned models include fewer fact recall-related parameters than Stage-tuned models.

Results. As shown in Figure 2 (a), mixed training yields more shared parameters than two-stage training across all values of k . For $k < 10^5$, it achieves $\frac{|S|}{k} > 0.6$, indicating that its shared parameters are stronger influenced by both BIO and QA than other parameters. At $k = 10^8$, shared parameters comprise fewer than 2% of all model parameters, and their total count is 1.2 times larger under mixed training than two-stage training. Figure 2 (b) shows the impact of shared parameters ($S_I \cup S_{II}$) on the QA out-of-distribution set when $k = 10^8$. Ablating them leads to a significant accuracy drop in the Mix-tuned model compared to the Stage-tuned model (66.0 vs. 6.7), indicating their functional impact. Pythia models exhibit consistent patterns, as shown in Appendix A.4.1. Appendix A.4.2 confirms that ablating an equal number of randomly selected parameters does not result in a comparable performance drop, validating the specificity and importance of shared parameters. These findings demonstrate that two-stage training and mixed training produce distinct sets of shared parameters, which directly influence fact recall performance.

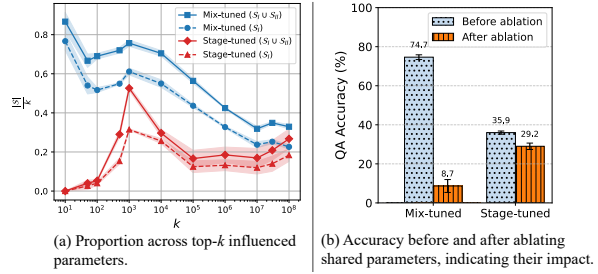


Figure 2: Shared parameters (S) in Llama: distribution and impact. (a) Mixed training yields more shared parameters than two-stage training. (b) Mix-tuned models show a larger accuracy drop after ablation, demonstrating their impact.

3.2 Comparing shared parameters across training strategies: mixed vs. two-stage training

The previous section highlights the impact of shared parameters on fact recall generalization. However, it remains unclear how these parameters function differently in Mix-tuned versus Stage-tuned models. Here, we empirically test this by measuring the contribution of shared parameters to fact recall.

Approach. Although our LMs are fully fine-tuned for the fact recall task, they still contain many parameters that may not be directly relevant. To reduce interference from such parameters, we aim to locate a sparse subset sufficient to recover fact recall performance, which we refer to as **fact recall-related parameters**. We then examine the role of shared parameters S within this subset to test their contribution. Specifically, we ablate S by resetting their values to the pre-trained state before identifying the fact recall-related subset. If shared parameters are functionally important, ablating them should significantly reduce the performance recovered by the localized subset. Moreover, if their roles differ across training strategies, their presence within the fact recall-related set should also differ between Mix-tuned and Stage-tuned models.

To locate fact recall-related parameters, we adopt the grafting approach from [42]. We define a binary mask $\gamma \in \{0, 1\}^{|\theta^{\text{task}}|}$, where $\gamma_i = 1$ indicates that parameter θ_i is included in the fact recall-related subset. The grafted model $\bar{\theta}^{\text{task}}$ is constructed by grafting γ -selected parameters from θ^{task} onto θ^{Pre} :

$$\bar{\theta}^{\text{task}}(\gamma) = \gamma \odot \theta^{\text{task}} + (1 - \gamma) \odot \theta^{\text{Pre}}, \quad (5)$$

where \odot denotes element-wise product. Figure 3 (a) illustrates this procedure.

Table 1: **Accuracy of grafted models using top- α parameters to recover the original fine-tuned models.** Grafted Mix-tuned models achieve stronger or comparable fact recall with fewer top parameters than grafted Stage-tuned models. Retaining shared parameters (\mathcal{S}) before grafting yields greater gains for Mix-tuned models. “w/o \mathcal{S} ” ablates shared parameters before grafting; “w/ \mathcal{S} ” retains them. Values in parentheses (e.g., +59.3) indicate accuracy gains over the w/o setting.

Setting	QA In-Distribution				QA Out-of-Distribution			
	α (%)	Accuracy (%)	$\frac{ \mathcal{S} \cap \gamma _0}{ \gamma _0}$ (%)	Recovery Rate (%)	α (%)	Accuracy (%)	$\frac{ \mathcal{S} \cap \gamma _0}{ \gamma _0}$ (%)	Recovery Rate (%)
Stage-tuned	—	100.0	—	100.0	—	35.6	—	100.0
Grafted w/ \mathcal{S}	0.50	96.1 (+59.3)	3.9	96.1	0.180	33.0 (+27.6)	5.9	92.7
Grafted w/o \mathcal{S}	0.50	36.8	0	36.8	0.180	5.4	0	15.1
Mix-tuned	—	98.3	—	100.0	—	74.7	—	100.0
Grafted w/ \mathcal{S}	0.10	93.5 (+60.1)	11.0	95.1	0.135	69.9 (+58.2)	9.3	93.6
Grafted w/o \mathcal{S}	0.10	33.4	0	33.9	0.135	11.7	0	15.7

We optimize γ to minimize the fact recall loss $\mathcal{L}_\tau(\overline{\theta^{\text{task}}}(\gamma))$ while maintaining sparsity. Since γ is non-differentiable, following [42], we relax it into continuous space as:

$$\arg \min_{\mathcal{B} \in \mathbb{R}^{|\theta^{\text{task}}|}} \mathcal{L}_\tau(\overline{\theta^{\text{task}}}(\gamma)), \quad (6)$$

$$\text{where } \gamma := \gamma_{\text{base}} \odot (1 - \sigma(\mathcal{B})) + (1 - \gamma_{\text{base}}) \odot \sigma(\mathcal{B}),$$

where $\sigma(\cdot)$ is the sigmoid function, \mathcal{B} is a real-valued vector, and γ_{base} is initialized using the top- α parameters based on the movement $|\theta^{\text{task}} - \theta^{\text{Pre}}|$. Here, α controls the initial sparsity level. This formulation ensures that the optimized γ deviates minimally from γ_{base} while minimizing task loss. Each active parameter in γ is thus associated with at least one factual triple (s, r, a) .

Experimental Setup. We applied the grafting procedure to both Mix-tuned and Stage-tuned models. To reduce computational cost, for both the QA in-distribution and out-of-distribution settings, we separately used 1,000 individuals to optimize the parameter mask γ and evaluate the grafted model $\overline{\theta^{\text{task}}}(\gamma)$. The loss \mathcal{L}_τ was computed over predicted attributes using questions as inputs. α was tuned over $[0, 100\%]$ to identify the smallest subset of parameters needed to recover the original performance. Implementation details and α -tuning curves are provided in Appendix A.5.1. For identifying the shared parameter set $\mathcal{S} = \mathcal{S}_I \cup \mathcal{S}_{II}$, we chose $k = 10^8$. Since this value offers a considerable number of shared parameters, we adopt it as a simple default for analyzing the role of \mathcal{S} , rather than searching for an optimal k . We also verified the consistency, robustness, and effectiveness of the grafting approach in Appendix A.5.2. We adopted *recovery rate* for evaluation, defined as the ratio between the grafted model’s accuracy and the original accuracy: $F(\overline{\theta^{\text{task}}}(\gamma))/F(\theta^{\text{task}})$.

Results. Table 1 shows grafting results on Llama. With $\alpha \leq 0.5\%$, all grafted models recover over 92.7% of their full fine-tuned accuracy, demonstrating effective localization of fact recall-related parameters. We observe three key differences between Mix-tuned and Stage-tuned models: (1) Mix-tuned models achieve higher $\frac{|\mathcal{S} \cap \gamma|_0}{|\gamma|_0}$, indicating a higher proportion of shared parameters within their fact recall-related subsets. (2) Figure 3 (b) further confirms that Mix-tuned models are more parameter-efficient, requiring fewer parameters to match or exceed the performance of Stage-tuned models. (3) Mix-tuned models rely more heavily on shared parameters: grafting with \mathcal{S} yields greater gains than without, and ablating \mathcal{S} alone on the out-of-distribution set nearly eliminates fact recall. This highlights the central role of shared parameters in enabling parameter-efficient recall. Pythia exhibits similar behavior, as detailed in Appendix A.5.3. We conclude that **mixed training yields more numerous and functionally efficient shared parameters than two-stage training, thereby teaching knowledge and supporting generalizable fact recall.**

4 Understanding shared parameters for fact recall: distribution in critical components

The previous section has answered our first question by showing that differences in shared parameters account for the fact recall performance gap between mixed training and two-stage training. In this section, we address our second question: *how does shared parameters internally support the model after mixed training for fact recall?* Previous studies have shown that attention heads and MLP neurons play critical roles in enabling final predictions—for example, attention heads enrich subject

representations [19], while MLP neurons calibrate output confidence [31]. This motivates us to analyze whether shared parameters are concentrated in the most critical attention heads and MLP neurons for fact recall. We hypothesize that components with relatively more shared parameters play more important functional roles. To systematically test this hypothesis, we adopt the framework of circuit theory, which identifies the most critical components in a network for a given task. Following prior studies [13, 44, 49], we conceptualize a *fact recall circuit* as a connected, directed acyclic subgraph $\mathcal{G} \in \{0, 1\}^{|N|}$ within the network, where N denotes the total number of nodes. Each node $n \in \mathcal{G}$ corresponds to a fine-grained attention head or an MLP neuron. (e.g., a query head in attention or an input projection neuron in an MLP layer). This fact recall circuit \mathcal{G} is expected to support fact recall in the grafted model $\theta^{\text{task}}(\gamma)$ using a minimal set of nodes. Our goal is to investigate whether shared parameters are concentrated in the minimal sufficient subgraph and most critical nodes of \mathcal{G} that enable fact recall. Formally, we represent the circuit model defined by the subgraph \mathcal{G} as:

$$\overline{\rho^{\text{task}}}(\mathcal{G}) = \mathcal{G} \odot \overline{\theta^{\text{task}}}(\gamma) + (1 - \mathcal{G}) \odot \theta^{\text{Pre}}, \quad (7)$$

where both $\overline{\theta^{\text{task}}}(\gamma)$ and θ^{Pre} are interpreted at the node level. Each element of \mathcal{G} determines whether the corresponding node is retained from $\overline{\theta^{\text{task}}}(\gamma)$ (element=1) or ablated into θ^{Pre} (element=0).

To search for the minimal sufficient subgraph and most critical nodes, we perform interventions:

1. **Forward Intervention (Discovering Sufficiency).** We initialize $\mathcal{G} = \{0\}^{|N|}$ and gradually flip elements of \mathcal{G} from 0 to 1 according to a predefined priority metric. During this process, we observe the resulting performance of $\overline{\rho^{\text{task}}}(\mathcal{G})$ to identify the minimal sufficient nodes.
2. **Backward Intervention (Discovering Necessity).** In contrast, we initialize $\mathcal{G} = \{1\}^{|N|}$ and progressively flip elements from 1 to 0, again guided by node priorities. This intervention reveals which nodes are most critical for maintaining fact recall performance.

To test whether nodes with more shared parameters play more critical roles in fact recall, we define the metric *Shared Size*, which prioritizes nodes by their shared parameter count. We evaluate its effectiveness against two baselines: *Random*, which assigns priorities randomly. *Grafted Size*, which prioritizes nodes by their number of fact recall-related parameters.

4.1 Concentration of shared parameters in critical attention heads: enabling fact recall

A straightforward approach to detect whether shared parameters concentrate in critical attention heads and MLP neurons would be to intervene on both simultaneously. However, prior work [15, 37] suggests that factual knowledge in pretrained Transformers is primarily stored in specific knowledge neurons. If this holds in our setting, jointly intervening both attention and MLP components could entangle recall and storage mechanisms, making it difficult to isolate the contribution of each. To avoid this, we treat MLP neurons as a knowledge base—a simplifying assumption motivated by prior work and preliminary evidence (Appendix A.6.1). Based on this insight, this section focuses exclusively on attention heads. We first formally define attention heads as follows.

Let the MHA module at layer ℓ consist of m heads. Let $\mathbf{x}_i^\ell \in \mathbb{R}^d$ denote the input representation of the i -th token for the MHA block at layer ℓ . The output \mathbf{o}_i^ℓ of the MHA module at layer ℓ is:

$$\mathbf{o}_i^\ell = W_O^\ell \cdot \text{Concat}(\mathbf{h}_i^{\ell,1}, \dots, \mathbf{h}_i^{\ell,m}) = \sum_{b=1}^m W_O^{\ell,b} \cdot \mathbf{h}_i^{\ell,b}, \quad (8)$$

$$\mathbf{h}_i^{\ell,b} = \sum_j \text{softmax}\left((\mathbf{q}_i^{\ell,b})^\top \mathbf{k}_j^{\ell,b}\right) \mathbf{v}_j^{\ell,b}, \quad (9)$$

$$\text{where } \mathbf{q}_i^{\ell,b} = W_Q^{\ell,b} \mathbf{x}_i^\ell, \quad \mathbf{k}_j^{\ell,b} = W_K^{\ell,b} \mathbf{x}_j^\ell, \quad \mathbf{v}_j^{\ell,b} = W_V^{\ell,b} \mathbf{x}_j^\ell.$$

$W_Q^{\ell,b}, W_K^{\ell,b}, W_V^{\ell,b} \in \mathbb{R}^{d_{\text{head}} \times d}$ are the query, key, and value projection matrices of head b . $W_O^{\ell,b} \in \mathbb{R}^{d \times d_{\text{head}}}$ is the output projection for head b from the full output matrix $W_O^\ell \in \mathbb{R}^{d \times m d_{\text{head}}}$. For fine-grained analysis, we define each projection matrix $W^{\ell,b} \in \{W_Q^{\ell,b}, W_K^{\ell,b}, W_V^{\ell,b}, W_O^{\ell,b}\}$ as the parameter of a fine-grained attention head and treat it as a node.

Experimental Setup. We performed interventions on the grafted Mix-tuned Llama and Pythia models, both optimized on the QA out-of-distribution set. Intervention effectiveness was evaluated

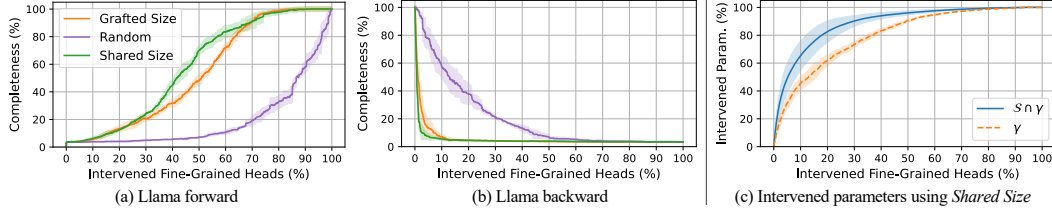


Figure 4: **Intervention results on fine-grained attention heads.** The *Shared Size* metric most effectively identifies minimal sufficient heads in (a) and most critical heads in (b) for fact recall circuits. (c) shows the corresponding fraction of intervened parameters.

on the QA out-of-distribution set using the same 1,000 individuals used in the original grafting experiments. We computed *completeness* for evaluation, defined as the proportion of accuracy retained by the circuit relative to the accuracy of the grafted model: $F(\rho^{\text{task}}(\gamma))/F(\theta^{\text{task}}(\gamma))$. For both shared parameters and fact recall-related parameters, we recorded their fraction of intervened parameters relative to the total in attention heads of θ^{task} , to observe their distribution.

Results. Figure 4 shows the intervention results. Among all metrics, *Shared Size* most effectively identifies both minimal sufficient and most critical heads, while *Random* performs the worst. Figure 4 (a) shows that *Shared Size* achieves over 80% completeness using only 60% of the fine-grained heads in Llama, outperforming *Grafted Size*, which reaches only 70% under the same condition. Figure 4 (c) reveals that these top 60% of heads identified by *Shared Size* account for over 95% of shared parameters in attention layers. Moreover, more than 60% of shared parameters are concentrated in the top 10% of heads. As shown in Figure 4 (b), ablating these top 10% of heads causes a performance drop of over 90%, highlighting their critical role. Pythia exhibits similar trends (Appendix A.7.1). These findings are consistent with our results on MLP neurons (Figures 15 and 16, Appendix A.6.2): over 30% of shared parameters in MLP neurons are concentrated in just 320 MLP neurons, and ablating these neurons causes a performance drop of over 60%. Taken together, these results confirm that **shared parameters are concentrated in critical heads and neurons that enable fact recall.**

4.2 Attention mechanisms induced by shared parameters: a case study

Previous sections have quantitatively shown that shared parameters support fact recall and are concentrated in critical attention heads. Here, we present a case study to qualitatively explore their semantic contribution—what functions these heads support. We examine the output head with the most shared parameters in the grafted Mix-tuned Llama model. Specifically, the output projection of Layer 21, Head 17 (L21H17) ranks second in shared parameter count, indicating its importance for fact recall. To better understand its role, we visualize its attention distribution and output logits. As shown in Figure 5, L21H17 exhibits interpretable and consistent attention patterns across BIO and QA inputs. Using the logit lens [39], we find that the subword “bl”—part of the subject’s name *Alexandra Leblanc*—appears among the top logits in both cases, aligning with the *Subject Linking* pattern, where the final token attends to “bl” in context. In contrast, in the grafted Stage-tuned model, L21H17 ranks only 17th in shared parameter count, indicating a weaker role in fact recall. This model also fails to recall the correct attribute for the same individual. As shown in Figure 19 (Appendix A.7.2), its attention is more diffuse and lacks clear alignment between BIO and QA. The output logits also differ: “BL” is top-ranked for QA input, while “department” is top-ranked for BIO. These findings suggest that mixed training encourages shared parameters to concentrate in attention heads that support reusable mechanisms across fact-storing and fact-recalling examples.

5 Related work

Mechanistic interpretability aims to explain model behavior by uncovering its internal mechanisms [22, 36, 45, 51]. Prior work has investigated how MLP neurons [22, 23, 46] and attention heads [44, 51] contribute to particular linguistic or reasoning tasks. Other studies have explored whether models develop internal capabilities aligned with human-interpretable concepts, such as geometry [24], monotonicity [26], or linearity [18, 27]. Various tools, including the logit lens [39] and path patching [50], have also been developed. Recent work has analyzed how different optimization

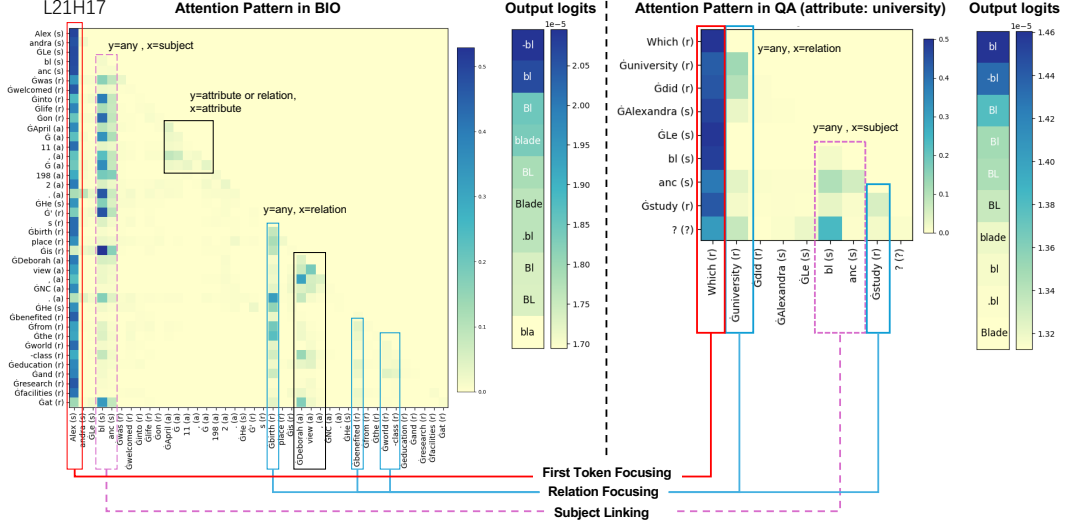


Figure 5: **Attention pattern of grafted Mix-tuned Llama in Layer 21, Head 17.** Left: attention pattern and output logits for the BIO input: *Alexandra Leblanc was welcomed into life on April 11, 1982...* Right: attention pattern and logits for the QA input from the same individual, whose QA is out-of-distribution. The model successfully recalls the attribute *Andrew Jackson University*. Colored rectangles highlight consistent attention behaviors across BIO and QA (e.g., purple = subject linking, blue = relation focusing). Output logits are computed by mapping the output states of the final token to the vocabulary space. A zoomed-in view is shown in the Figure 18, Appendix A.7.2.

strategies affect a model’s internal capabilities [28, 43]. Our work contributes to this by introducing a tool, *cross-task gradient trace*, to analyze why mixed training teaches knowledge. Rather than focusing on specific components, we study a small set of parameters that support this function.

Instruction-tuning [41] fine-tunes LMs on (INSTRUCTION, OUTPUT) pairs. We adopt this setup for QA-tuning. Subsequent work has explored alternative data sources [34, 47, 52], tuning strategies [6, 8, 11], tuned-LMs [14, 16], and evaluation [1, 12]. We focus on interpreting one variant of instruction-tuning: *mixed training* [3], which jointly trains on statements and instructions.

Understanding factual knowledge in language models falls into two main directions: understanding how models *store* facts [15, 25, 26, 30, 35, 49], and how they *recall* facts [3, 4, 19, 20, 40]. For storing, [49] identify specific attention heads, named *mover heads*, that propagate factual information from fact-storing examples for downstream storage. For recalling, [19] show that *extract heads* and MLP blocks work together to recall facts, and [49] further find that the identified *mover heads* also function as *extract heads* during fact recall. [20] show that generalization in fact recall correlates with how well facts are stored. While these works imply overlapping parameters for fact-storing and fact-recalling from the perspective of attention heads and model performance, this study provides the first empirical evidence by analyzing *shared parameters*: those strongly influenced by both fact-storing and fact-recalling examples.

6 Conclusion

In this work, we introduce a tool *cross-task gradient trace* to investigate why two-stage training encourages memorization but mixed training teaches knowledge. Our experimental results reveal that **mixed training teaches knowledge by increasing both the quantity and collective importance of shared parameters compared to two-stage training. Moreover, in Mix-tuned models, these shared parameters are concentrated in critical attention heads involved in fact recall.** These findings not only show that shared parameters are essential for generalization, but also highlight their ability to uncover the minimal sufficient and most critical heads and neurons that form a fact recall circuit. Given the efficiency and interpretability of shared parameters, future work may explore whether similar mechanisms emerge in other cross-task settings. The proposed tool is model-agnostic and readily extensible for such investigations.

References

- [1] Vaibhav Adlakha, Parishad BehnamGhader, Xing Han Lu, Nicholas Meade, and Siva Reddy. Evaluating correctness and faithfulness of instruction-following models for question answering. *Transactions of the Association for Computational Linguistics*, 12:681–699, 2024.
- [2] Meta AI. Llama 3.2: Revolutionizing edge ai and vision with open, customizable models. <https://ai.meta.com/blog/llama-3-2-connect-2024-vision-edge-mobile-devices/>, 2024.
- [3] Zeyuan Allen-Zhu and Yuanzhi Li. Physics of language models: Part 3.1, knowledge storage and extraction. In *International Conference on Machine Learning*, pages 1067–1077. PMLR, 2024.
- [4] Zeyuan Allen-Zhu and Yuanzhi Li. Physics of language models: Part 3.2, knowledge manipulation. In *International Conference on Learning Representations*, 2025.
- [5] Marco Ancona, Enea Ceolini, Cengiz Öztireli, and Markus Gross. Towards better understanding of gradient-based attribution methods for deep neural networks. In *International Conference on Learning Representations*, 2018.
- [6] Yuntao Bai, Andy Jones, Kamal Ndousse, Amanda Askell, Anna Chen, Nova DasSarma, Dawn Drain, Stanislav Fort, Deep Ganguli, Tom Henighan, et al. Training a helpful and harmless assistant with reinforcement learning from human feedback. *arXiv preprint arXiv:2204.05862*, 2022.
- [7] Stella Biderman, Hailey Schoelkopf, Quentin Gregory Anthony, Herbie Bradley, Kyle O’Brien, Eric Hallahan, Mohammad Aflah Khan, Shrivanshu Purohit, Usven Sai Prashanth, Edward Raff, Aviya Skowron, Lintang Sutawika, and Oskar Van Der Wal. Pythia: A suite for analyzing large language models across training and scaling. In *International Conference on Machine Learning*, pages 2397–2430. PMLR, 2023.
- [8] Tim Brooks, Aleksander Holynski, and Alexei A Efros. Instructpix2pix: Learning to follow image editing instructions. In *Conference on Computer Vision and Pattern Recognition (CVPR)*, pages 18392–18402. IEEE, 2023.
- [9] Lawrence Chan, Adria Garriga-Alonso, Nicholas Goldowsky-Dill, Ryan Greenblatt, Jenny Nitishinskaya, Ansh Radhakrishnan, Buck Shlegeris, and Nate Thomas. Causal scrubbing: A method for rigorously testing interpretability hypotheses. In *AI Alignment Forum*, volume 2, 2022.
- [10] Yuheng Chen, Pengfei Cao, Yubo Chen, Kang Liu, and Jun Zhao. Journey to the center of the knowledge neurons: Discoveries of language-independent knowledge neurons and degenerate knowledge neurons. In *Proceedings of the AAAI Conference on Artificial Intelligence*, volume 38, pages 17817–17825, 2024.
- [11] Daixuan Cheng, Yuxian Gu, Shaohan Huang, Junyu Bi, Minlie Huang, and Furu Wei. Instruction pre-training: Language models are supervised multitask learners. In *Proceedings of the 2024 Conference on Empirical Methods in Natural Language Processing*, pages 2529–2550. Association for Computational Linguistics, 2024.
- [12] Hyung Won Chung, Le Hou, Shayne Longpre, Barret Zoph, Yi Tay, William Fedus, Yunxuan Li, Xuezhi Wang, Mostafa Dehghani, Siddhartha Brahma, Albert Webson, Shixiang Shane Gu, Zhuyun Dai, Mirac Suzgun, Xinyun Chen, Aakanksha Chowdhery, Alex Castro-Ros, Marie Pellat, Kevin Robinson, Dasha Valter, Sharan Narang, Gaurav Mishra, Adams Yu, Vincent Y. Zhao, Yanping Huang, Andrew M. Dai, Hongkun Yu, Slav Petrov, Ed H. Chi, Jeff Dean, Jacob Devlin, Adam Roberts, Denny Zhou, Quoc V. Le, and Jason Wei. Scaling instruction-finetuned language models. *Journal of Machine Learning Research*, 25:70:1–70:53, 2024.
- [13] Arthur Conmy, Augustine Mavor-Parker, Aengus Lynch, Stefan Heimersheim, and Adrià Garriga-Alonso. Towards automated circuit discovery for mechanistic interpretability. In *Advances in Neural Information Processing Systems*, pages 16318–16352, 2023.

- [14] Mike Conover, Matt Hayes, Ankit Mathur, Jianwei Xie, Jun Wan, Sam Shah, Ali Ghodsi, Patrick Wendell, Matei Zaharia, and Reynold Xin. Free dolly: Introducing the world’s first truly open instruction-tuned llm, 2023.
- [15] Damai Dai, Li Dong, Yaru Hao, Zhifang Sui, Baobao Chang, and Furu Wei. Knowledge neurons in pretrained transformers. In *Proceedings of the 60th Annual Meeting of the Association for Computational Linguistics*, pages 8493–8502. Association for Computational Linguistics, 2022.
- [16] Wenliang Dai, Junnan Li, Dongxu Li, Anthony Tiong, Junqi Zhao, Weisheng Wang, Boyang Li, Pascale Fung, and Steven Hoi. InstructBLIP: Towards general-purpose vision-language models with instruction tuning. In *Advances in Neural Information Processing Systems*, 2023.
- [17] DeepSeek-AI. Deepseek-v3 technical report. *arXiv preprint arXiv:2412.19437*, 2024.
- [18] Joshua Engels, Eric J Michaud, Isaac Liao, Wes Gurnee, and Max Tegmark. Not all language model features are one-dimensionally linear. In *International Conference on Learning Representations*, 2025.
- [19] Mor Geva, Jasmijn Bastings, Katja Filippova, and Amir Globerson. Dissecting recall of factual associations in auto-regressive language models. In *Proceedings of the 2023 Conference on Empirical Methods in Natural Language Processing*, pages 12216–12235. Association for Computational Linguistics, 2023.
- [20] Gaurav Rohit Ghosal, Tatsunori Hashimoto, and Aditi Raghunathan. Understanding finetuning for factual knowledge extraction. In *International Conference on Machine Learning*, pages 15540–15558. PMLR, 2024.
- [21] Olga Golovneva, Zeyuan Allen-Zhu, Jason E Weston, and Sainbayar Sukhbaatar. Reverse training to nurse the reversal curse. In *Conference on Language Modeling*, 2024.
- [22] Wes Gurnee, Theo Horsley, Zifan Carl Guo, Tara Rezaei Kheirkhah, Qinyi Sun, Will Hathaway, Neel Nanda, and Dimitris Bertsimas. Universal neurons in GPT2 language models. *Transactions on Machine Learning Research*, 2024.
- [23] Wes Gurnee, Neel Nanda, Matthew Pauly, Katherine Harvey, Dmitrii Troitskii, and Dimitris Bertsimas. Finding neurons in a haystack: Case studies with sparse probing. *Transactions on Machine Learning Research*, 2023.
- [24] Wes Gurnee and Max Tegmark. Language models represent space and time. In *International Conference on Learning Representations*, 2024.
- [25] Benjamin Heinzerling and Kentaro Inui. Language models as knowledge bases: On entity representations, storage capacity, and paraphrased queries. In *Proceedings of the 16th Conference of the European Chapter of the Association for Computational Linguistics*, pages 1772–1791. Association for Computational Linguistics, 2021.
- [26] Benjamin Heinzerling and Kentaro Inui. Monotonic representation of numeric attributes in language models. In *Proceedings of the 62nd Annual Meeting of the Association for Computational Linguistics*, pages 175–195. Association for Computational Linguistics, 2024.
- [27] Evan Hernandez, Arnab Sen Sharma, Tal Haklay, Kevin Meng, Martin Wattenberg, Jacob Andreas, Yonatan Belinkov, and David Bau. Linearity of relation decoding in transformer language models. In *International Conference on Learning Representations*, 2024.
- [28] Samyak Jain, Robert Kirk, Ekdeep Singh Lubana, Robert P. Dick, Hidenori Tanaka, Tim Rocktäschel, Edward Grefenstette, and David Krueger. Mechanistically analyzing the effects of fine-tuning on procedurally defined tasks. In *International Conference on Learning Representations*, 2024.
- [29] Zhengbao Jiang, Zhiqing Sun, Weijia Shi, Pedro Rodriguez, Chunting Zhou, Graham Neubig, Xi Lin, Wen-tau Yih, and Srini Iyer. Instruction-tuned language models are better knowledge learners. In *Proceedings of the 62nd Annual Meeting of the Association for Computational Linguistics*, pages 5421–5434. Association for Computational Linguistics, 2024.

- [30] Shahar Katz, Yonatan Belinkov, Mor Geva, and Lior Wolf. Backward lens: Projecting language model gradients into the vocabulary space. In *Proceedings of the 2024 Conference on Empirical Methods in Natural Language Processing*, pages 2390–2422. Association for Computational Linguistics, 2024.
- [31] Vedang Lad, Wes Gurnee, and Max Tegmark. The remarkable robustness of LLMs: Stages of inference? In *ICML 2024 Workshop on Mechanistic Interpretability*, 2024.
- [32] Jiwei Li, Will Monroe, and Dan Jurafsky. Understanding neural networks through representation erasure. *arXiv preprint arXiv:1612.08220*, 2016.
- [33] Xiyu Liu, Zhengxiao Liu, Naibin Gu, Zheng Lin, Wanli Ma, Ji Xiang, and Weiping Wang. Relation also knows: Rethinking the recall and editing of factual associations in auto-regressive transformer language models. In *Proceedings of the 39th Annual AAAI Conference on Artificial Intelligence*, 2025.
- [34] Shayne Longpre, Le Hou, Tu Vu, Albert Webson, Hyung Won Chung, Yi Tay, Denny Zhou, Quoc V Le, Barret Zoph, Jason Wei, et al. The flan collection: Designing data and methods for effective instruction tuning. In *International Conference on Machine Learning*, pages 22631–22648. PMLR, 2023.
- [35] Pratyush Maini, Michael Curtis Mozer, Hanie Sedghi, Zachary Chase Lipton, J Zico Kolter, and Chiyuan Zhang. Can neural network memorization be localized? In *International Conference on Machine Learning*, pages 23536–23557. PMLR, 2023.
- [36] Samuel Marks and Max Tegmark. The geometry of truth: Emergent linear structure in large language model representations of true/false datasets. In *Conference on Language Modeling*, 2024.
- [37] Kevin Meng, David Bau, Alex Andonian, and Yonatan Belinkov. Locating and editing factual associations in gpt. In *Advances in Neural Information Processing Systems*, pages 17359–17372, 2022.
- [38] Jingcheng Niu, Andrew Liu, Zining Zhu, and Gerald Penn. What does the knowledge neuron thesis have to do with knowledge? In *International Conference on Learning Representations*, 2024.
- [39] nostalgebraist. Interpreting gpt: the logit lens. <https://www.lesswrong.com/posts/AcKRB8wDpdAN6v6ru/interpreting-gpt-the-logit-lens>, 2020.
- [40] Francesco Ortu, Zhijing Jin, Diego Doimo, Mrinmaya Sachan, Alberto Cazzaniga, and Bernhard Schölkopf. Competition of mechanisms: Tracing how language models handle facts and counterfactuals. In *Proceedings of the 62nd Annual Meeting of the Association for Computational Linguistics*, pages 8420–8436. Association for Computational Linguistics, 2024.
- [41] Long Ouyang, Jeffrey Wu, Xu Jiang, Diogo Almeida, Carroll Wainwright, Pamela Mishkin, Chong Zhang, Sandhini Agarwal, Katarina Slama, Alex Ray, John Schulman, Jacob Hilton, Fraser Kelton, Luke Miller, Maddie Simens, Amanda Askell, Peter Welinder, Paul F Christiano, Jan Leike, and Ryan Lowe. Training language models to follow instructions with human feedback. In *Advances in Neural Information Processing Systems*, pages 27730–27744, 2022.
- [42] Abhishek Panigrahi, Nikunj Saunshi, Haoyu Zhao, and Sanjeev Arora. Task-specific skill localization in fine-tuned language models. In *International Conference on Machine Learning*, pages 27011–27033. PMLR, 2023.
- [43] Aleksandar Petrov, Philip Torr, and Adel Bibi. When do prompting and prefix-tuning work? a theory of capabilities and limitations. In *International Conference on Learning Representations*, 2024.
- [44] Nikhil Prakash, Tamar Rott Shaham, Tal Haklay, Yonatan Belinkov, and David Bau. Fine-tuning enhances existing mechanisms: A case study on entity tracking. In *International Conference on Learning Representations*, 2024.

- [45] Elena Voita, Javier Ferrando, and Christoforos Nalmpantis. Neurons in large language models: Dead, n-gram, positional. In *Findings of the Association for Computational Linguistics: ACL 2024*, pages 1288–1301. Association for Computational Linguistics, 2024.
- [46] Xiaozhi Wang, Kaiyue Wen, Zhengyan Zhang, Lei Hou, Zhiyuan Liu, and Juanzi Li. Finding skill neurons in pre-trained transformer-based language models. In *Proceedings of the 2022 Conference on Empirical Methods in Natural Language Processing*, pages 11132–11152. Association for Computational Linguistics, 2022.
- [47] Yizhong Wang, Swaroop Mishra, Pegah Alipoormolabashi, Yeganeh Kordi, Amirreza Mirzaei, Atharva Naik, Arjun Ashok, Arut Selvan Dhanasekaran, Anjana Arunkumar, David Stap, Eshaan Pathak, Giannis Karamanolakis, Haizhi Lai, Ishan Purohit, Ishani Mondal, Jacob Anderson, Kirby Kuznia, Krma Doshi, Kuntal Kumar Pal, Maitreya Patel, Mehrad Moradshahi, Mihir Parmar, Mirali Purohit, Neeraj Varshney, Phani Rohitha Kaza, Pulkit Verma, Ravsehaj Singh Puri, Rushang Karia, Savan Doshi, Shailaja Keyur Sampat, Siddhartha Mishra, Sujan Reddy A, Sumanta Patro, Tanay Dixit, and Xudong Shen. Super-NaturalInstructions: Generalization via declarative instructions on 1600+ NLP tasks. In *Proceedings of the 2022 Conference on Empirical Methods in Natural Language Processing*, pages 5085–5109. Association for Computational Linguistics, 2022.
- [48] An Yang, Baosong Yang, Beichen Zhang, Binyuan Hui, Bo Zheng, Bowen Yu, Chengyuan Li, Dayiheng Liu, Fei Huang, Haoran Wei, Huan Lin, Jian Yang, Jianhong Tu, Jianwei Zhang, Jianxin Yang, Jiaxi Yang, Jingren Zhou, Junyang Lin, Kai Dang, Keming Lu, Keqin Bao, Kexin Yang, Le Yu, Mei Li, Mingfeng Xue, Pei Zhang, Qin Zhu, Rui Men, Runji Lin, Tianhao Li, Tianyi Tang, Tingyu Xia, Xingzhang Ren, Xuancheng Ren, Yang Fan, Yang Su, Yichang Zhang, Yu Wan, Yuqiong Liu, Zeyu Cui, Zhenru Zhang, and Zihan Qiu. Qwen2.5 technical report. *arXiv preprint arXiv:2412.15115*, 2024.
- [49] Yunzhi Yao, Ningyu Zhang, Zekun Xi, Mengru Wang, Ziwen Xu, Shumin Deng, and Huajun Chen. Knowledge circuits in pretrained transformers. In *Advances in Neural Information Processing Systems*, 2024.
- [50] Fred Zhang and Neel Nanda. Towards best practices of activation patching in language models: Metrics and methods. In *International Conference on Learning Representations*, 2024.
- [51] Yiran Zhao, Wenxuan Zhang, Guizhen Chen, Kenji Kawaguchi, and Lidong Bing. How do large language models handle multilingualism? In *Advances in Neural Information Processing Systems*, 2024.
- [52] Chunting Zhou, Pengfei Liu, Puxin Xu, Srini Iyer, Jiao Sun, Yuning Mao, Xuezhe Ma, Avia Efrat, Ping Yu, LILI YU, Susan Zhang, Gargi Ghosh, Mike Lewis, Luke Zettlemoyer, and Omer Levy. LIMA: Less is more for alignment. In *Advances in Neural Information Processing Systems*, 2023.

A Appendix / supplemental material

A.1 Limitations and Broader Impacts

Impacts. This paper proposes a model-agnostic tool, *cross-task gradient trace*, for analyzing factual behavior in LMs. As this tool can identify the most critical attention heads and MLP neurons across tasks, further interpretation of these components—e.g., using other analysis tools—may reveal memorized data. Such interpretability can help LM developers audit and protect critical components from potential misuse, but it also raises the risk of exposing sensitive information that should remain inaccessible, such as personal data or passwords. To mitigate this risk, one possible solution is to anonymize or mask sensitive content in advance.

Limitations. While our work offers a strong empirical foundation for understanding the effect of mixed training on fact recall in LMs, several limitations remain for future exploration: 1. Model Scope. Our analysis is limited to two text-only LMs with approximately 3 billion parameters. It remains to be seen whether the observed patterns generalize to larger or multimodal models, such as those incorporating image or video inputs. 2. Data Realism. The datasets used are synthetic,

clean, and balanced. Real-world data often involve noise, imbalance, and outdated or conflicting information, especially across fact-storing and fact-recalling inputs. Future work could evaluate the robustness of mixed training under these more realistic conditions. 3. Mechanistic Insight. While we quantitatively demonstrate the role of shared parameters, this paper stops short of a detailed causal analysis of how these parameters improve the fine-tuned model. Deeper understanding of the underlying mechanisms could guide better model and training design. We view this paper as a foundational step toward understanding fact recall in LMs. Despite the above limitations, our current analyses offer a solid platform for future work in model interpretability, training strategies, and cross-task generalization.

A.2 Details on data preparation

A.2.1 BIO dataset

This research followed the general setup of [3] with some modifications to generate synthetic datasets. Specifically, we generated profiles for $N = 10,000$ individuals. For each person, we independently and randomly sampled their first and last name, gender, birth date, birth city, attended university, job, employer, and blood type from uniform distributions. Details are as follows:

- First and last names were drawn from pools of 400 and 1000 English names, respectively. Each of the 10,000 individuals had a unique full names to ensure disambiguation during fact recall.
- Birth dates were generated with years from 1900 to 2099, months from 1 to 12, and days from 1 to 28.
- Birth cities were selected from a pool of 200 fake cities, each randomly assigned to one of 56 U.S. state abbreviations. Birth cities were formatted as, e.g., Amyville, GA.
- Attended Universities were selected from a list of 300 U.S. higher education institutions.
- Jobs were draw from a pool of 100 occupations (e.g., chartered public finance accountant).
- Employers were selected from a pool of 263 fake Companies (e.g., Bell, Ramos and Romero).
- Blood types were sampled from the standard 8 blood types, including A+, A-, B+, B-, AB+, AB-, O+, O-.
- Genders was selected as either F or M.

We used the Faker Python module to generate the pools of names, cities, jobs, and employers. For each individual, we generated one biographical entry consisting of six sentences, each corresponding to one attribute, and the entry maintained a consistent order: birth date, birth city, attended university, job, employer, and blood type. Each sentence was instantiated from a randomly selected template. Specifically, we used 21 templates for birth dates, 33 for birth cities, 22 for universities, 24 for jobs, 29 for employers, and 21 for blood types. Pronouns (she/he) were assigned based on the individual’s gender (F/M). Example biographies:

- *Brandon Horne’s life journey began on February 1, 2089. She spent her youth in Cindyborough, AL. She developed a passion for learning at University of North Texas Health Science Center at Fort Worth. She had embraced a career as a landscape architect. She accepted a leadership position at Bell, Ramos and Romero. She is classified as having blood AB+.*
- *Meghan Charles’s birthday is remembered on November 10, 2092. He took birth in Amyville, GA. He took advantage of the diverse programs offered at Cedar Crest College. He was involved in work as a chartered public finance accountant. He aligned his professional ambitions with Henson, Ellis and Sexton. He has a blood type of O-.*

To evaluate BIO accuracy, we used part of the biography as a prompt and asked the model to generate the corresponding attribute. Accuracy was measured as the proportion of exact matches. Example:

- Prompt: Brandon Horne’s life journey began on February 1, 2089. She spent her youth in
- Attribute: Cindyborough, AL.

A.2.2 QA dataset

For each individual, we generated six fixed questions corresponding to the six attributes. The question served as the prompt, and the model generated the attribute as the answer. Accuracy was again computed by exact match. Examples:

- *What is the birth date of Meghan Charles? November 10, 2092.*
- *What is the birth city of Meghan Charles? Amyville, GA.*
- *Which university did Meghan Charles study? Cedar Crest College.*
- *What is the job of Meghan Charles ? chartered public finance accountant.*
- *Which company did Meghan Charles work for?" Henson, Ellis and Sexton.*
- *What is the blood type of Meghan Charles ? O-.*

A.3 Details on BIO/QA fine-tuning

We fine-tuned all models using the AdamW optimizer with an initial learning rate of 0.0001 and cosine learning rate decay on NVIDIA A100 40GB. All models were trained with next-token prediction. For BIO fine-tuning and mixed training, we used a linear warm-up of 1,600 steps and a batch size of 32. For QA fine-tuning, we used no warm-up and a batch size of 256. Table 2 summarizes the total number of training updates for each model setting. The estimated total GPU compute time in fine-tuning models is 281.22 hours without taking preliminary or failed experiments (that didn’t make it into the paper) into consideration.

Table 2: Training updates for different model and training strategies.

Model	Training Type	Updates	Training Hours (1 run)
Llama	BIO	6,820	10.37
	QA	400	4.36
	Mix	10,571	22.16
Pythia	BIO	13,981	18.27
	QA	800	6.15
	Mix	19,437	32.43

Figure 6 shows the performance of fine-tuned models. Both the QA-tuned and Mix-tuned models perform well on data seen during training. Specifically, they retain biographical facts (BIO Accuracy $\geq 88.7\%$) and adapt well to the question-answer format (QA in_dist accuracy $\geq 98.1\%$). However, the QA-tuned model struggles to generalize to novel questions in QA out_dist. In contrast, the Mix-tuned model maintains strong performance (over 48.9% accuracy) on the unseen QA set, demonstrating superior generalization.

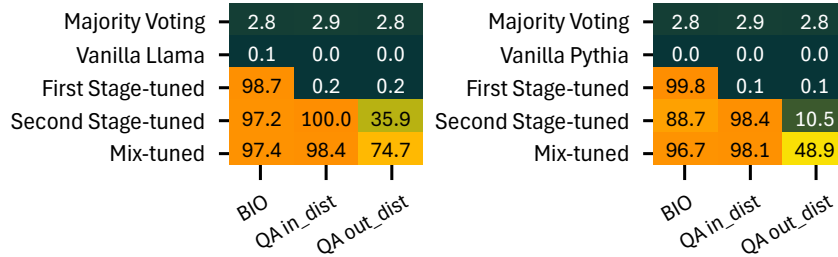


Figure 6: **Performance of fine-tuned Llama and Pythia on BIO, QA in-distribution, and QA out-of-distribution sets.** High accuracy on BIO and QA in-distribution sets indicates successful retention of biographical facts and adaptation to the question-answer format, respectively.

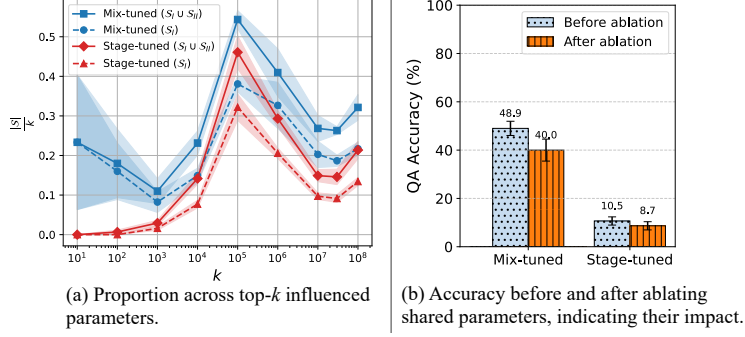


Figure 7: Shared parameters (\mathcal{S}) in Pythia: distribution and impact.

A.4 Details on shared parameters

A.4.1 Distribution and impact of shared parameters on Pythia models.

Figure 7 shows the distribution and impact of shared parameters in Pythia models. As shown in Figure 7 (a), mixed training yields more shared parameters than two-stage training across k . When $k = 10^8$, the shared set is 1.5 times larger under mixed training. Figure 7 (b) shows the impact of shared parameters on the QA out-of-distribution set, when $\mathcal{S} = \mathcal{S}_I \cup \mathcal{S}_{II}$ and $k = 10^8$. Ablating them leads to a larger accuracy drop in the Mix-tuned model compared to the Stage-tuned model (8.9 vs. 1.8), indicating their functional impact.

A.4.2 Comparison between shared parameters and random parameters

Figure 8 shows the ablation results for shared parameters ($\mathcal{S} = \mathcal{S}_I \cup \mathcal{S}_{II}$) when $k = 10^8$ on the BIO, QA in-distribution, and QA out-of-distribution sets.

To validate the importance of shared parameters, we conducted an ablation study using randomly selected parameters as a control. Specifically, we randomly sampled the same number of parameters as the shared parameters identified when $k = 10^8$, and ablated them by resetting their values in θ^{task} to their original pre-trained values in θ^{pre} . We denote these randomly sampled parameters as \mathcal{S}' . Figure 9 shows that ablating these random parameters leads to negligible changes in model performance, in contrast to the significant drop observed when ablating shared parameters in Figure 8. This confirms the specific importance of shared parameters in supporting fact recall.

Llama ($\mathcal{S} \in \theta^{\text{Task}} \leftarrow \mathcal{S} \in \theta^{\text{Pre}}$)				Pythia ($\mathcal{S} \in \theta^{\text{Task}} \leftarrow \mathcal{S} \in \theta^{\text{Pre}}$)			
Stage-tuned	92.3 (-4.9)	95.1 (-4.9)	29.2 (-6.7)	73.1 (-15.6)	80.6 (-17.8)	8.7 (-1.8)	
Mix-tuned	11.5 (-85.9)	19.8 (-78.6)	8.7 (-66.0)	87.3 (-9.4)	91.5 (-6.6)	40.0 (-8.9)	
	BIO	QA in_dist	QA out_dist	BIO	QA in_dist	QA out_dist	

Figure 8: **Accuracy after ablating shared parameters \mathcal{S} .** Values in parentheses (e.g., -0.0) denote accuracy differences computed as ablated minus original.

Llama ($\mathcal{S}' \in \theta^{\text{Task}} \leftarrow \mathcal{S}' \in \theta^{\text{Pre}}$)				Pythia ($\mathcal{S}' \in \theta^{\text{Task}} \leftarrow \mathcal{S}' \in \theta^{\text{Pre}}$)			
Stage-tuned	97.2 (-0.0)	100.0 (-0.0)	36.1 (+0.2)	88.9 (+0.2)	98.4 (-0.0)	10.6 (+0.1)	
Mix-tuned	97.4 (-0.0)	98.4 (-0.0)	74.9 (+0.2)	96.6 (-0.1)	98.0 (-0.1)	48.9 (-0.0)	
	BIO	QA in_dist	QA out_dist	BIO	QA in_dist	QA out_dist	

Figure 9: **Accuracy after ablating random parameters \mathcal{S}' .** Values in parentheses (e.g., -0.0) denote accuracy differences computed as ablated minus original.

A.5 Details on grafting

A.5.1 Experimental setup

For all grafting experiments, we optimized each model using SGD with a batch size 2, a learning rate 10^8 , and a training time of 24 hours on NVIDIA A100 40GB. The optimization stopped early if $|\gamma|_0 > 1.5\alpha$ or if the accuracy exceeds 0.97. Both the embedding and final projection layers were excluded from grafting by removing them from the initial mask γ_{base} . Figure 10 presents the tuning curves of α . The selected α values were chosen to ensure that the grafted models recovered approximately 92–97% of the performance of the fully fine-tuned models. The estimated total GPU compute time in our grafting experiments is 2712 hours without taking preliminary or failed experiments (that didn’t make it into the paper) into consideration.

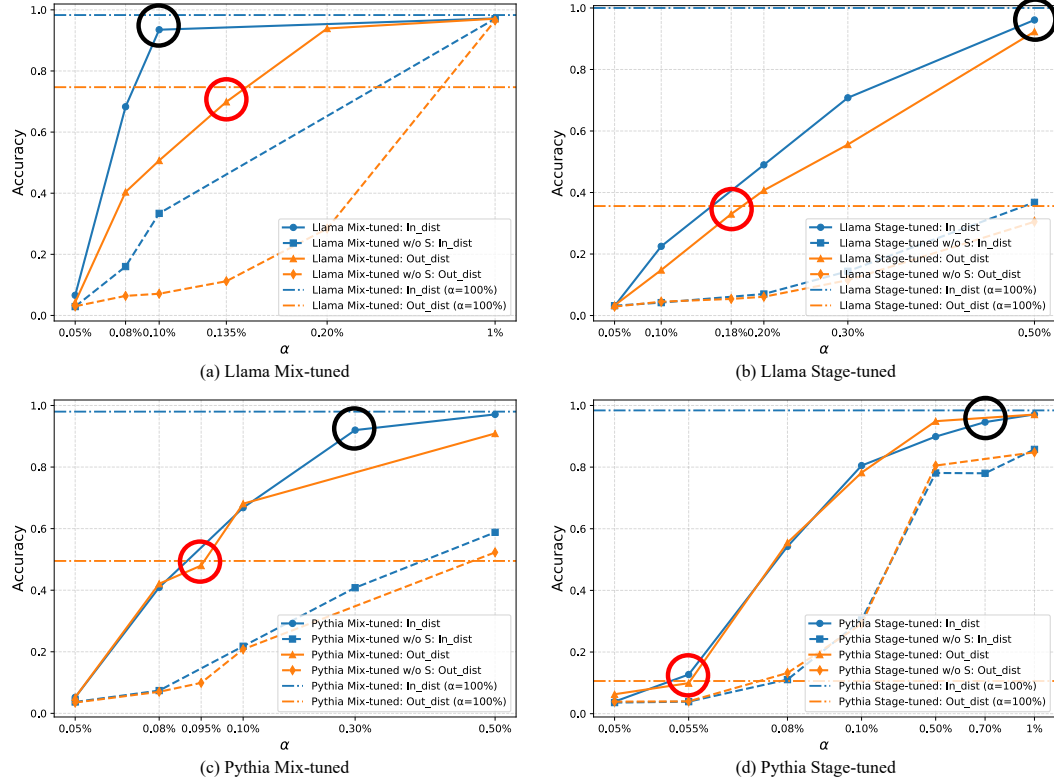


Figure 10: Tuning curves of α for various models. Red circles indicate the selected α for QA out-of-distribution settings; black circles indicate those for QA in-distribution.

A.5.2 Consistency, robustness and effectiveness of grafting

Setting. We tested *grafting* with 1,000 individuals from the BIO dataset using the Mix-tuned LLaMA model. To estimate the relationship $\gamma_1 \subseteq \gamma_2$ when $|\gamma_1|_0 < |\gamma_2|_0$, we calculated the overlapping ratio as $|\gamma_1 \cap \gamma_2|_0 / |\gamma_1|_0$.

Run 1	Run 2	Run 3	Mean (std)
97.43	97.08	97.05	97.19 (0.2113)

(a) BIO Acc. vs. different run

	Run 1	Run 2	Run 3
Run 1	100.00	98.87	98.88
Run 2	98.87	100.00	98.89
Run 3	98.88	98.89	100.00

(b) Overlapping Ratio vs. different run

Figure 11: Robustness of grafting with different random seeds.

Robustness. We verify that grafting results are stable across different random seeds. As shown in Figure 11 for $\alpha = 1\%$, grafting achieves consistent accuracy (std = 0.2113) and high overlap across seeds ($\geq 98.87\%$).

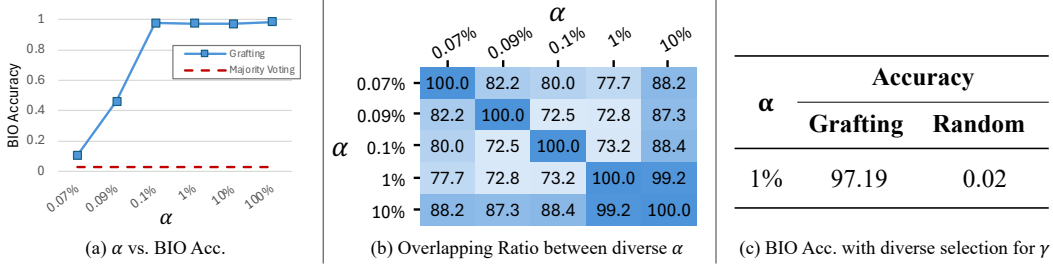


Figure 12: Consistency and Effectiveness of using grafting to locate γ .

Consistency. We expect a consistent inclusion relation among masks γ for different α : if $\alpha_1 < \alpha_2$, then $\gamma_1 \subseteq \gamma_2$. For any pair of α from Figure 12 (a), Figure 12 (b) shows that the overlap is $\geq 72.5\%$, confirming consistency.

Effectiveness. Grafting should yield better performance than random parameter selection. For comparison, we randomly selected parameter subsets and report the averaged Acc. over three runs. As shown in Figure 12 (c), grafting outperforms random selection by 97.17 points, highlighting its effectiveness.

A.5.3 Grafting results on Pythia

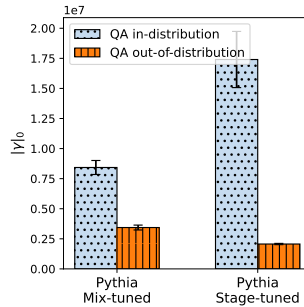


Figure 13: Number of fact recall-related parameters (γ) in grafted Pythia models.

Table 3: **Accuracy of grafted Pythia models using top- α parameters to recover the original fine-tuned Pythia models.** “w/o S ” ablates shared parameters before grafting; “w/ S ” retains them. Values in parentheses (e.g., +16.6) indicate accuracy gains over the w/o setting.

Setting	QA In-Distribution				QA Out-of-Distribution			
	α (%)	Accuracy (%)	$\frac{ S \cap \gamma _0}{ \gamma _0}$ (%)	Recovery Rate (%)	α (%)	Accuracy (%)	$\frac{ S \cap \gamma _0}{ \gamma _0}$ (%)	Recovery Rate (%)
Stage-tuned	—	98.4	—	100.0	—	10.6	—	100.0
Grafted w/ S	0.70	94.6 (+16.6)	1.9	96.2	0.055	9.9 (+5.9)	7.0	93.2
Grafted w/o S	0.70	78.0	0	79.2	0.055	4.0	0	38.1
Mix-tuned	—	98.0	—	1.000	—	49.5	—	100.0
Grafted w/ S	0.30	92.0 (+51.2)	5.4	94.0	0.095	48.0 (+38.1)	8.3	96.9
Grafted w/o S	0.30	40.8	0	41.7	0.095	9.9	0	20.1

Figure 13 and Table 3 show the grafting results on Pythia models. With $\alpha \leq 0.7\%$, all grafted models recover over 93.2% of their full fine-tuned accuracy, demonstrating effective localization of fact recall-related parameters. We observe the same three key differences between Mix-tuned and Stage-tuned models as Llama models: (1) Mix-tuned models achieves higher $\frac{|S \cap \gamma|_0}{|\gamma|_0}$. (2) Mix-tuned models require fewer fact recall-related parameters to match or exceed the performance of Stage-tuned

models. (3) Mix-tuned models rely more heavily on shared parameters: grafting with \mathcal{S} yields greater gains than without, and ablating \mathcal{S} alone on the out-of-distribution set nearly eliminates fact recall.

A.6 Details on MLP neurons

We formally define the structure of MLP neurons within the Transformer architecture. Let $\mathbf{x}_i^\ell \in \mathbb{R}^d$ denote the input representation of the i -th token for the MLP block at layer ℓ , where d is the hidden size. In Llama, the MLP block at layer ℓ computes:

$$\mathbf{m}_i^\ell = W_{\text{down}}^\ell \left[\phi \left(W_{\text{gate}}^\ell \mathbf{x}_i^\ell \right) \odot \left(W_{\text{up}}^\ell \mathbf{x}_i^\ell \right) \right], \quad (10)$$

$$\text{where } W^\ell \mathbf{x}_i^\ell = \sum_{b=1}^d \mathbf{w}^{\ell,b} \cdot x_i^{\ell,b},$$

where ϕ is a nonlinear activation function (*e.g.*, SiLU). The matrices $W_{\text{up}}^\ell, W_{\text{gate}}^\ell \in \mathbb{R}^{d_i \times d}$ and $W_{\text{down}}^\ell \in \mathbb{R}^{d \times d_i}$ are learnable parameters of the MLP block at layer ℓ , with d_i as the intermediate dimension. $\mathbf{w}^{\ell,b}$ is the b -th column of W^ℓ and $x_i^{\ell,b}$ is the b -th component of \mathbf{x}_i^ℓ . We define each neuron as a single column vector in the down/up/gate matrices (*e.g.*, $\mathbf{w}_{\text{gate}}^{\ell,b}$), and treat it as an individual node. In Pythia, Equation (10) is simplified by removing $W_{\text{up}}^\ell \mathbf{x}_i^\ell$ term.

A.6.1 Neurons as knowledge base

Given an attribute a , we denote the set of intervention steps at which a is successfully predicted during forward intervention as $T = \{t_{j_1}, \dots, t_{j_{|T|}}\}$. We hypothesize that grafted MLP layers serve as a knowledge base: as the graph \mathcal{G} includes more grafted MLP neurons from $\overline{\theta^{\text{task}}}(\gamma)$, more attributes should be correctly predicted, and these predictions should be preserved across steps. In other words, information retrieved at earlier stages should be preserved until the final intervention step. Based on this assumption, to evaluate the grafted MLP neurons, we compute the following metrics for each successfully predicted attribute and report their average across all attributes:

- **Overall Continuity Ratio:** $|T|/(j_{|T|} - j_1 + 1)$. This quantifies the proportion of steps where the attribute are successfully predicted within its prediction window $j_{|T|} - j_1 + 1$.
- **Max Continuous Streak Ratio:** $|T'|/(j_{|T|} - j_1 + 1)$, where T' is the longest consecutive subsequence in T . This quantifies the longest continuous streak where the attribute are successfully predicted within its prediction window $j_{|T|} - j_1 + 1$.

We also evaluate **Final Retention Ratio**, denoted as the fraction of successfully recalled attribute at the final intervention step.

Table 4: Continuity analysis of correctly predicted attributes by grafted Mix-tuned models.

Model	Overall Continuity Ratio	Max Continuous Streak Ratio	Final Retention Ratio
Llama	0.9196	0.8074	0.9144
Pythia	0.7975	0.6344	0.8487

Experimental Setup. We conducted the forward intervention on MLP neurons using the *Shared Size* metric and observed predictions of $\overline{\rho^{\text{task}}}(\mathcal{G})$ during intervention. For efficiency, we intervened on 8,192 neurons per step.

Results. Table 4 reports results on the QA out-of-distribution set. Llama achieves higher continuity and retention metrics than Pythia. Both grafted Mix-tuned Llama and Pythia exhibit strong consistency: an overall continuity ratio ≥ 0.7975 , a max continuous streak ratio ≥ 0.6344 , and a final retention ratio ≥ 0.8487 . These findings support our hypothesis that grafted MLP layers act as a knowledge base. Figure 14 shows case studies.

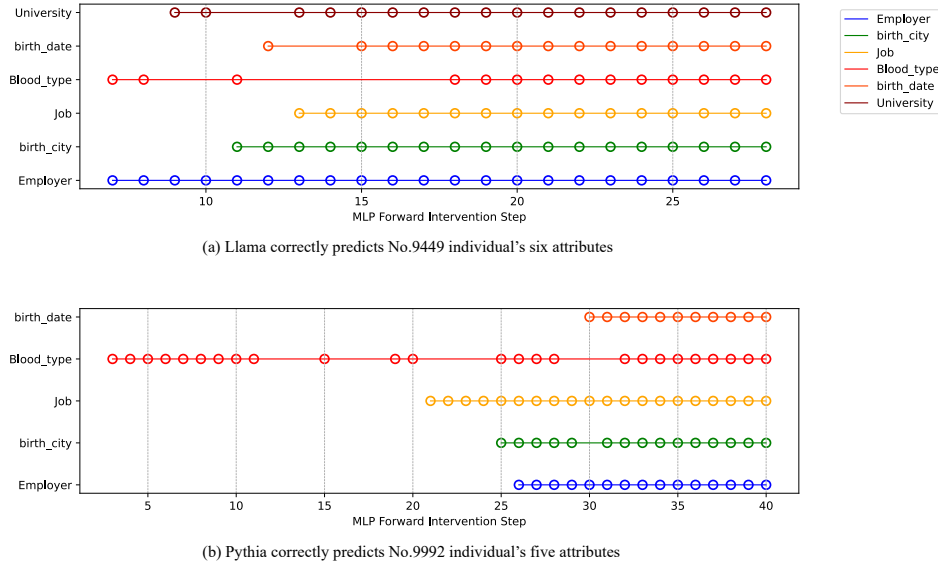


Figure 14: Case studies showing attribute prediction steps of grafted Mix-tuned models. Each marker **O** denotes a step where the corresponding attribute is correctly predicted.

A.6.2 Distribution of shared parameters in critical MLP neurons

Experimental Setup. We performed interventions on the grafted Mix-tuned Llama and Pythia models, both optimized on the QA out-of-distribution set. For all components other than MLP neurons, the corresponding node values in \mathcal{G} were fixed to 1 throughout the intervention. For computational efficiency, we intervened on 8,192 neurons per step in the forward direction and 64 neurons per step in the backward direction. Intervention effectiveness was evaluated on the QA out-of-distribution set using the same 1,000 individuals used in the original grafting experiments. We computed *completeness* for evaluation, defined as the proportion of accuracy retained by the circuit: $F(\rho^{\text{task}}(\gamma))/F(\theta^{\text{task}}(\gamma))$. We conducted the interventions on NVIDIA A100 40GB. Each step took approximately 1.5 minutes to execute. The estimated total GPU compute time for the MLP neuron interventions is 28.8 hours, excluding preliminary or failed runs that were not included in the paper.

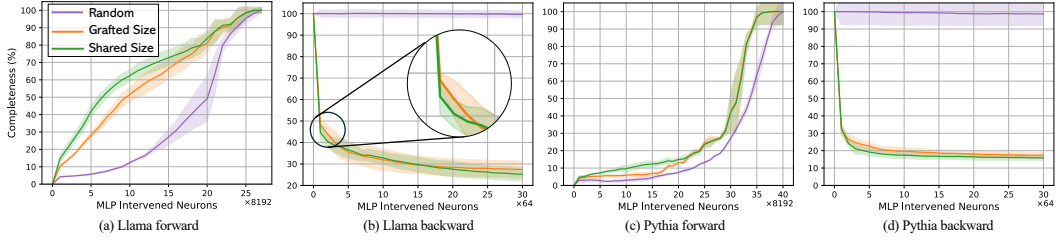


Figure 15: Forward and backward intervention results on MLP neurons. *Shared Size* metric most effectively identify critical MLP neurons.

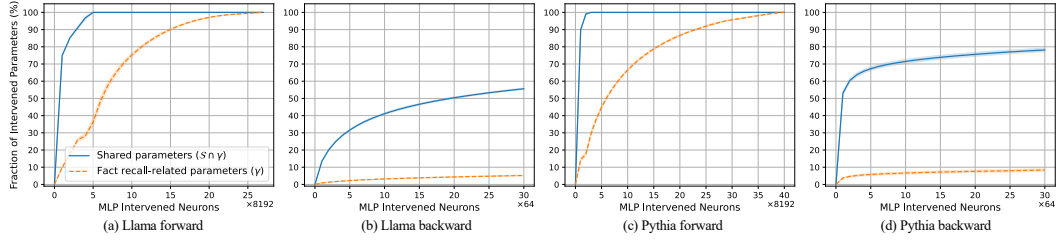


Figure 16: Fraction of intervened parameters in MLP neurons when using the *Shared Size* priority metric.

Results. Figure 15 presents the intervention results on MLP neurons. Figures 15 (a) and (c) show that almost all neurons in the grafted Mix-tuned models are necessary to recover the performance of θ^{task} , supporting the notion that MLP blocks serve as a factual knowledge base. Importantly, the *Shared Size* metric achieves higher completeness than the *Random* and *Grafted Size* metrics during early-to-middle forward intervention (steps 1–20). Additionally, Figures 15 (b) and (d) show that *Shared Size* consistently outperforms *Grafted Size* in identifying the most critical neurons. Ablating top 320 neurons leads to a performance drop of over 60%. Figures 16 (b) and (d) show that over 30% of shared parameters in MLP neurons are concentrated in these 320 neurons. Moreover, Figures 16 (a) and (c) show that 100% of shared parameters in MLP neurons are concentrated in top 40,960 neurons. This indicates that, during forward intervention, the neurons after 40,960 rank by *Shared Size* contains no shared parameters, and the performance increasing are brought by rest parameters. This suggests that while shared parameters are not required for most of the factual knowledge base (Appendix A.6.1), they are concentrated in critical neurons that enable fact recall behavior.

A.7 Details on attention heads

Experimental Setup. In Llama, the number of parameters in the query and output projections was three times larger than that in the key and value projections. In the Section 4.1, to balance their contributions, we multiplied the shared parameter and fact recall-related parameter counts of the key and value projections by a factor of 3. We intervene each fine-grained head at each intervention step. We conducted the interventions on NVIDIA A100 40GB. Each step took approximately 1.5 minutes to execute. The estimated total GPU compute time for the attention head interventions is 1612.8 hours, excluding preliminary or failed runs that were not included in the paper.

A.7.1 Distribution of shared parameters in critical attention heads in Pythia

Similar to the Llama models, Figure 17 shows that among all metrics, *Shared Size* most effectively identifies both minimal sufficient and most critical heads, while *Random* performs the worst. Figure 4 (a) shows that *Shared Size* achieves over 80% completeness using 80% of the fine-grained heads, outperforming *Grafted Size*, which reaches lower than 70% under the same condition. Figure 4(c) reveals that these top 80% of heads identified by *Shared Size* account for over 95% of shared parameters in attention layers. Moreover, more than 60% of these parameters are concentrated in the top 10% of heads. As shown in Figure 4 (b), ablating these heads causes a performance drop of over 90%. It demonstrates the robustness of *Shared Size* across LMs: in both Llama and Pythia, it consistently outperforms *Grafted Size* during middle-to-late interventions.

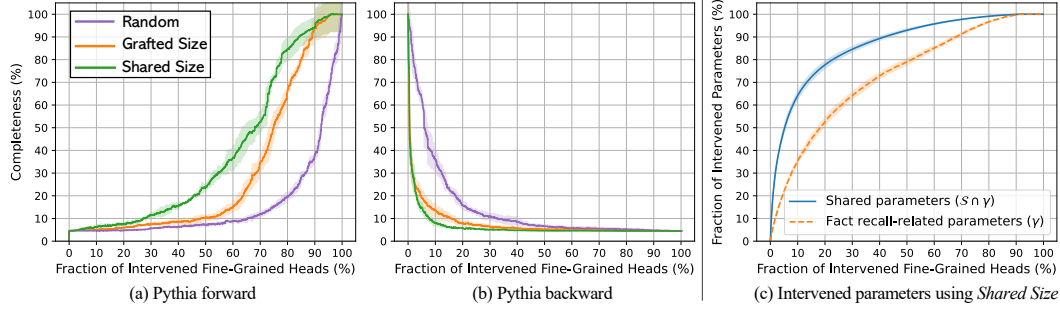


Figure 17: **Intervention results on fine-grained attention heads of Pythia models.** The *Shared Size* metric most effectively identifies minimal sufficient heads in (a) and most critical heads in (b) for fact recall circuits. (c) shows the corresponding fraction of intervened parameters.

A.7.2 Observed attention patterns

Figures 18 and 19 show the attention mechanisms of Layer 21, Head 17 in the grafted Mix-tuned and Stage-tuned Llama models, respectively. The output project of this head has the second largest shared parameter count in the Mix-tuned, while only 17th largest in the Stage-tuned model. While this head exhibits interpretable and consistent attention patterns across both BIO and QA inputs in the Mix-tuned model, it appears more diffuse and lacks clear alignment in the Stage-tuned model. The output logits also differ: the Mix-tuned model ranks “*bl*” highest for both BIO and QA, whereas the Stage-tuned model ranks “*department*” highest under BIO input and “*Bl*” under QA.

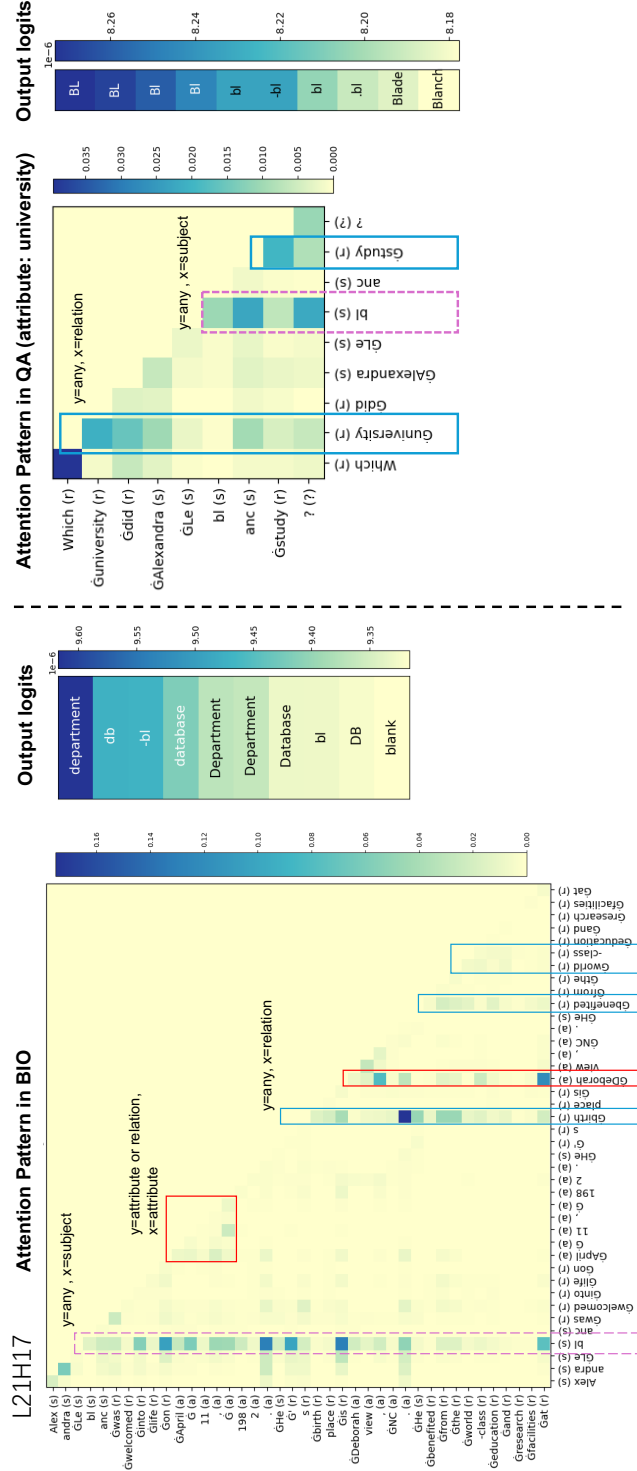


Figure 19: **Attention pattern of grafted Stage-tuned Llama in Layer 21, Head 17.** Left: attention pattern and output logits for the BIO input: *Alexandra Leblanc was welcomed into life on April 11, 1982. He ’s birthplace is Deborahview, NC. He benefited from the world-class education and research facilities at Andrew Jackson University. He served as a it sales professional. He became a part of innovative team at the company Long-Peters. He is a member of the blood group O+.* Right: attention pattern and logits for the QA input from the same individual, whose QA is out-of-distribution. The model **fails** to recall the attribute *Andrew Jackson University*. Colored rectangles highlight consistent attention behaviors as grafted Mix-tuned Llama. Output logits are computed by mapping the output states of the final token to the vocabulary space.